Inorg. Chem. **2005**, *44*, 6646–6654

Macrocyclic Lanthanide Complexes as Artificial Nucleases and Ribonucleases: Effects of pH, Metal Ionic Radii, Number of Coordinated Water Molecules, Charge, and Concentrations of the Metal Complexes

C. Allen Chang,* Bo Hong Wu, and Bu Yuan Kuan

Department of Biological Science and Technology, National Chiao Tung University, 75 Po-Ai Street, Hsinchu, Taiwan 30039, R. O. C.

Received October 18, 2004

We have been interested in the design, synthesis, and characterization of artificial nucleases and ribonucleases by employing macrocyclic lanthanide complexes because their high thermodynamic stability, low kinetic lability, high coordination number, and charge density (Lewis acidity) allow more design flexibility and stability. In this paper, we report the study of the use of the europium(III) complex, $EuDO2A^+$ (DO2A is 1,7-dicarboxymethyl-1,4,7,10-tetraazacyclododecane) and other lanthanide complexes (i.e., $LaDO2A^+$, $YbDO2A^+$, $EuK21DA^+$, $EuEDDA^+$, and EuHEDTA where K21DA is 1,7-diaza-4,10,13-trioxacyclopentadecane-*N*,*N*′-diacetic acid, EDDA is ethylenediamine-*N*,*N*′-diacetic acid, and HEDTA is N-hydroxyethyl-ethylenediamine-*N*,*N*′,*N*′-triacetic acid), as potential catalysts for the hydrolysis of the phosphodiester bond of BNPP (sodium bis(4-nitrophenyl)-phosphate). For the pH range 7.0–11.0 studied, $EuDO2A^+$ promotes BNPP hydrolysis with the quickest rates among $LaDO2A^+$, $EuDO2A^+$, and $YbDO2A^+$. This indicates that charge density is not the only factor affecting the reaction rates. Among the four complexes, $EuDO2A^+$, $EuK21DA^+$, $EuEDDA^+$, and EuHEDTA, with their respective number of inner-sphere coordinated water molecules three, two, five, and three, $EuEDDA^+$, with the greatest number of inner-sphere coordinated water molecules and a positive charge, promotes BNPP hydrolysis more efficiently at pH below 8.4, and the observed rate trend is $EuEDDA^+ > EuDO2A^+ > EuK21DA^+ >$ EuHEDTA. At pH > 8.4, the $EuEDDA^+$ solution becomes misty and precipitates form. At pH 11.0, the hydrolysis rate of BNPP in the presence of $EuDO2A^+$ is 100 times faster than that of EuHEDTA, presumably because the positively charged $EuDO2A^+$ is more favorable for binding with the negatively charged phosphodiester compounds. The logarithmic hydrolysis constants (pK_h) were determined, and are reported in the parentheses, by fitting the kinetic k_{obs} data vs pH for $EuDO2A^+$ (8.4), $LaDO2A^+$ (8.4), $YbDO2A^+$ (9.4), $EuK21DA^+$ (7.8), $EuEDDA^+$ (9.0), and EuHEDTA (10.1). The preliminary rate constant–$[EuDO2A^+]$ data at pH 9.35 were fitted to a monomer–dimer reaction model, and the dimer rate constant is 400 times greater than that of the monomer. The fact that $YbDO2A^+$ catalyzes BNPP less effectively than $EuDO2A^+$ is tentatively explained by the formation of an inactive dimer, $[Yb(DO2A)(OH)]_2$, with no coordination unsaturation for BNPP substrate binding.

Introduction

Natural nucleases, ribonucleases, and restriction enzymes have very specific and sometimes not well-separated substrate binding and catalytic domains and are not always readily useful for many nonphysiological applications, such as DNA/RNA sequence determination and production, gene expression control, and as effective therapeutic agents for many viral and genetic diseases. Artificial nucleases/ribonucleases with design flexibility such as separated substrate binding and cleavage domains, therefore, may provide several advantages.[1−3] A number of transition[4−15] and lanthanide (Ln)[16−36] metal ions as well as complexes and oligonucleotide derivatives have been reported to hydrolyze DNA/RNA or model compounds for such purposes.

Enzymatic hydrolysis of DNA usually follows two steps: (1) nucleophilic attack on a P atom (by, e.g., an OH^- ion)

(1) Bashkin, J. K.; Trawick, B. N.; Daniher. A. T. *Chem. Rev.* **1998**, *98*, 939−960.
(2) Oivanen, M.; Kuusela, S.; Lonnberg, H. *Chem. Rev.* **1998**, *98*, 961−990.
(3) Williams, N. H.; Takasaki, B.; Well, M.; Chin, J. *Acc. Chem. Res.* **1999**, *32*, 485−493.
(4) Gellman, S. H.; Petter, R.; Breslow, R. *J. Am. Chem. Soc.* **1986**, *108*, 2388−2394.

10.1021/ic0485458 CCC: $30.25
Published on Web 08/25/2005

forms a five-coordinate intermediate and (2) the removal of the 5′-OH and P−O bond breakage. The rate-determining step is proposed to be the second step, that is, P−O bond breakage.[37] In nonenzymatic hydrolysis, the P−O(3′) scission can also take place. On the other hand, RNA hydrolysis is 10^5-10^6 times faster than DNA because of the presence of a 2′-OH group which acts as an internal nucleophile. It was reported that trivalent lanthanide ions are the most effective for RNA hydrolysis,[38] and the reaction rates increase with increasing lanthanide atomic number. Although Ce(IV) was claimed to be the most effective DNA hydrolysis promoter, Tm(III), Yb(III), and Lu(III) were found to be the better RNA hydrolysis promoters.[37,38] Similar to DNA hydrolysis studies, it was claimed that during RNA hydrolysis, the bimetallic hydroxo cluster, $[Ln_2(OH)_2]^{4+}$, was the most effective species.[38] This is consistent with a report on rapid cleavage of RNA with a La(III) dimer, $[La_2(OH)_5^+]$.[25] However, because of the complex hydrolytic properties and potential Ln−hydroxide cluster formation of cationic lanthanide complexes, the design of efficient agents and the elucidation of possible mechanisms for their promotion of phosphodiester hydrolysis remain to be challenges.[3]

In addition to applications as artificial restriction enzymes, these macrocyclic lanthanide complex systems could also be potentially applied as reagents for pesticide and nerve gas hydrolysis involving phosphate or phosphonate ester bonds.

We have been interested in the understanding of the coordination chemistry of lanthanide complexes and the development of their biomedical applications[39−47] including their use as magnetic resonance imaging contrast agents,[48] luminescence probes,[49] and artificial nucleases/ribonucleases. In this paper, we report the effects of pH, lanthanide metal ionic radii, number of inner-sphere coordinated water molecules, charge, and concentration of the lanthanide metal complexes on the hydrolysis of a compound, BNPP (sodium bis(4-nitrophenyl)-phosphate), containing a phosphodiester bond. The ligands involved in this study are DO2A, K21DA, EDDA, and HEDTA, where DO2A is 1,7-dicarboxymethyl-1,4,7,10-tetraazacyclododecane, K21DA is 1,7-diaza-4,10,-13-trioxacyclopentadecane-*N*,*N*′-diacetic acid, EDDA is ethylenediamine-*N*,*N*′-diacetic acid, and HEDTA is *N*-hydroxyethyl-ethylenediamine-*N*,*N*′,*N*′-triacetic acid. The structural formulas of the $EuDO2A^+$, $EuK21DA^+$, and $EuEDDA^+$ complexes are shown in Scheme 1.

Experimental Section

Materials and Standard Solutions. Analytical reagent-grade chemicals and buffers, unless otherwise stated, were purchased from Sigma (St. Louis, MO), Aldrich (Milwaukee, WI), or Merck (Dammstadt, Germany) and were used as received without further

(5) Hettich, R.; Schneider, H.-J. *J. Am. Chem. Soc*. **1997**, *119*, 5638−5647.
(6) Sissi, C.; Rossi, P.; Felluga, F.; Formaggio, F.; Palumbo, M.; Tecilla, P.; Toniolo, C.; Scrimin, P. *J. Am. Chem. Soc*. **2001**, *123*, 3169−3170.
(7) Gajda, T.; Düpre, Y.; Török, I.; Harmer, J.; Schweiger, A.; Sander, J.; Kuppert, D.; Hegetschweiler, K. *Inorg. Chem.* **2001**, *40*, 4918−4927.
(8) Branum, M. E.; Tipton, A. K.; Zhu, S.; Que, L. *J. Am. Chem. Soc.* **2001**, *123*, 1898−1904.
(9) Liu, C.; Yu, S.; Li, D.; Liao, Z.; Sun, X.; Xu, H. *Inorg. Chem.* **2002**, *41*, 913−922.
(10) Deck, K. M.; Tseng, T. A.; Burstyn, J. N. *Inorg. Chem.* **2002**, *41*, 669−677.
(11) McCue, K. P.; Voss, D. A. Jr.; Marks, C.; Morrow, J. R. *J. Chem. Soc., Dalton Trans.* **1998**, 2961−2963.
(12) McCue, K. P.; Morrow, J. R. *Inorg. Chem*. **1999**, *38*, 6136−6142.
(13) Iranzo, O.; Elmer, T.; Richard, J. P.; Morrow, J. *Inorg. Chem*. **2003**, *42*, 7737−7746.
(14) Iranzo, O.; Richard, J. P.; Morrow, J. *Inorg. Chem*. **2004**, *43*, 1743−1750.
(15) Arca, M.; Bencini, A.; Berni, E.; Caltagirone, C.; Devillanova, F. A.; Isaia, F.; Garau, A.; Giorgi, C.; Lippolis, V.; Perra, A.; Tei, L.; Valtancoli, B. *Inorg. Chem*. **2003**, *42*, 6929−6939.
(16) Breslow, R.; Huang, D.-L. *Proc. Natl. Acad. Sci. U.S.A.* **1991**, 4080−4083.
(17) Morrow, J. R.; Buttrey, L. A.; Shelton, V. L.; Berback, K. A. *J. Am. Chem. Soc*. **1992**, *114*, 1903−1905.
(18) Amin, S.; Morrow, J. R.; Lake, C. H.; Churchill, M. R. *Angew. Chem., Int. Ed. Engl*. **1994**, *33*, 773−775.
(19) Takasaki, B. K.; Chin, J. *J. Am. Chem. Soc*. **1994**, *116*, 1121−1122.
(20) Sumaoka, I.; Miyama, S.; Komiyama, M. *J. Chem. Soc., Chem. Commun.* **1994**, 1755−1756.
(21) Matsuda, S.; Endo, M.; Komiyama, M. *J. Chem. Soc., Chem. Commun.* **1994**, 2019−2020.
(22) Magda, D.; Miller, R. A.; Sessler, J. L.; Iverson, B. L. *J. Am. Chem. Soc*. **1994**, *116*, 7439−7440.
(23) Hall, J.; Husken, D.; Pieles, U.; Moser, H. E.; Haner, R. *Chem. Biol*. **1994**, *1*, 185−190.
(24) Rammo, J.; Hettich, R.; Roigk, A.; Schneider, H.-J. *J. Chem. Soc., Chem. Commun*. **1996**, 105−107.
(25) Hurst, P.; Takasaki, B. K.; Chin, J. *J. Am. Chem. Soc*. **1996**, *118*, 9982−9983.
(26) Amin, S.; Voss, D. A., Jr.; Horrocks, W. D., Jr.; Morrow, J. R. *Inorg. Chem*. **1996**, *35*, 7466−7467.
(27) Baker, B. F.; Khalili, H.; Wei, N.; Morrow, J. R. *J. Am. Chem. Soc.* **1997**, *119*, 8749−8755.
(28) Chappell, I. L.; Voss, D. A. Jr.; Horrocks, W. D., Jr.; Morrow, J. R. *Inorg. Chem.* **1998**, *37*, 3989−3998.
(29) Roigk, A.; Hettich, R.; Schneider, H.-J. *Inorg. Chem*. **1998**, *37*, 751−756.
(30) Roigk, A.; Yescheulova, O. V.; Fedorov, Y. V.; Fedorova, O. A.; Gromov, S. P.; Schneider, H.-J. *Org. Lett.* **1999**, *1*, 833−835.
(31) Jurek, P. E.; Jurek, A. M.; Martell, A. E. *Inorg. Chem.* **2000**, *39*, 1016−1020.
(32) Epstein, D. M.; Chappell, L. L.; Khalili, H.; Supkowski, R. M.; Horrocks, W. D., Jr.; Morrow, J. R. *Inorg. Chem.* **2000**, *39*, 2130−2134.
(33) Bligh, S. W. A.; Choi, N.; Evagorou, E. G.; McPartlin, M.; White, K. N. *J. Chem. Soc., Dalton Trans.* **2001**, 3169−3172.
(34) Gómez-Tagle, P.; Yatsimirsky, A. K. *Inorg. Chem.* **2001**, *40*, 3786−3796.
(35) Gómez-Tagle, P.; Yatsimirsky, A. K. *J. Chem. Soc., Dalton Trans.* **2001**, 2663−2670.
(36) Gunnlaugsson, T.; Davies, R. J. H.; Nieuwenhuyzen, M.; Stevenson, C. S.; Viguier, R.; Mulready, S. *J. Chem. Soc., Chem. Commun.* **2002**, 2136−2137.
(37) Komiyama, M.; Tekeda, H.; Shigekawa, H. *J. Chem. Soc., Chem. Commun*. **1999**, 1443−1451.
(38) Endo, M.; Azuma, Y.; Saga, Y.; Kuzuta, G.; Kawai, M.; Komiyama, M. *J Org. Chem*. **1997**, *62*, 846−852.
(39) Chang, C. A.; Rowland, M. E. *Inorg. Chem*. **1983**, *22*, 3866−3869.
(40) Chang, C. A.; Sekhar, V. C. *Inorg. Chem*. **1986**, *25*, 2061−2065.
(41) Chang, C. A.; Ochaya, V. O. *Inorg. Chem*, **1986**, *25*, 355−358.
(42) Chang, C. A.; Sekhar, V. C. *Inorg. Chem*. **1987**, *26*, 1981−1985.
(43) Holz, R. C.; Klakamp, S. L.; Chang, C. A.; Horrocks, W. D., Jr. *Inorg. Chem.* **1990**, *29*, 2651−2658.
(44) Chang, C. A.; Francesconi, L. C.; Malley, M. F.; Kumar, K.; Gougoutas, J. Z.; Tweedle, M. F.; Lee, D. W.; Wilson, L. J. *Inorg. Chem*. **1993**, *32*, 3501−3508.
(45) Chang, C. A. *Proc. Natl. Sci. Counc., Repub. China, Part A: Phys. Sci. Eng*. **1997**, *21*, 1−13.
(46) Chang, C. A.; Shieh, F.-K.; Liu, Y.-L.; Chen, Y.-H.; Chen, H.-Y.; Chen, C.-Y. *J. Chem. Soc., Dalton Trans.* **1998**, 3243−3248.
(47) Chang, C. A.; Liu, Y.-L.; Chen, C.-Y.; Chou, X.-M. *Inorg. Chem*. **2001**, *40*, 3448−3455.
(48) Caravan, P.; Ellison, J. J.; McMurry, T. J.; Lauffer, R. B. *Chem. Rev.* **1999**, *99*, 2293.
(49) Lehn, J. M. Roth, C. O. *Helv. Chim. Acta* **1991**, *74*, 572.

Scheme 1. Structural Formulas of $EuDO2A^+$, $EuK21DA^+$, and $EuEDDA^+$ Complexes

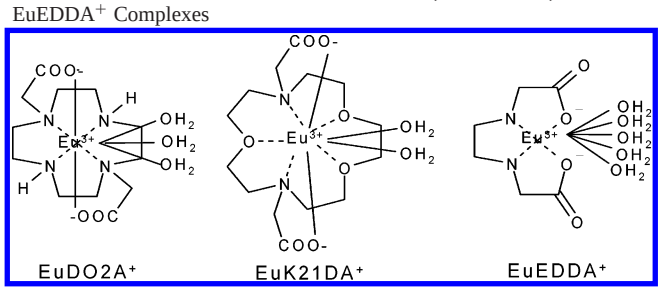

purification. Disodium ethylenediaminetetraacetic acid (EDTA) was purchased from Fisher. The ligands DO2A.2HCl·H_2O[46] and K21DA[41] were prepared and purified according to a published method with minor modifications. Microanalysis was performed for DO2A. Anal. Calcd for $C_{12}H_{24}N_4O_4$·2HCl·H_2O: C, 38.00; H, 7.44; N, 14.77. Found: C, 37.98; H, 7.24; N, 14.71. Carbonate-free deionized water was used for all of the solution preparations.

The concentration of DO2A stock solution (ca. 0.01 M) was determined by acid−base titration using a standard tetramethylammonium hydroxide solution (0.1 M) and was also checked by complexometric back-titration.[39] The concentrations of the lanthanide nitrate stock solutions were ca. 0.01 M and were standardized by EDTA titration using xylenol orange as the indicator. The EDTA solution was standardized by titrating a calcium carbonate primary standard solution (first dissolved in HCl solution) at pH 10 using calmagite as the indicator.

The 0.1 M tetramethylammonium hydroxide solution was prepared by diluting a 20% $(CH_3)_4NOH$−methanol solution obtained from Aldrich (carbonate free). The aqueous $(CH_3)_4NOH$ solution was standardized by using reagent grade potassium hydrogen phthalate. A 0.1 M HCl solution was prepared by diluting reagent-grade HCl to ca. 1 M, then diluting the 1 M solution to 0.1 M. This solution was standardized by using the standard $(CH_3)_4NOH$ solution. A 1.0 M stock solution of tetramethylammonium chloride (Aldrich) was prepared and diluted to 0.1 M for each titration to maintain a constant ionic strength (0.1 M, charge unit neglected).

Potentiometric Titrations. Acid−base and complex formation titrations were carried out at a constant ionic strength of 0.10 M $(CH_3)_4NCl$ using reported procedures.[39] These titrations were used to determine the ligand purity by checking the inflection points and by calculating the ligand protonation constants and to aid in the preparation of lanthanide complex solutions. A model 720 Metrohm titroprocessor in conjunction with a Metrohm Combination electrode was employed to monitor the pH. Generally, the ligand concentration was 1−2 mM, and the metal ion concentration was in slight excess (~2%) Under this experimental condition, only 1:1 complexes were formed between each ligand and metal ion. The ionic strength of the solution was adjusted to 0.1 M using 1 M $(CH_3)_4NCl$. The $(CH_3)_4NOH$ solution was delivered from a 10-mL automatic Brinkmann Metrohm model 665 Dosimat buret with a reading accuracy of ±0.001 mL.

Kinetic Measurements. All of the lanthanide complex solutions were freshly prepared by mixing 1.00:1.02 metal salt/ligand molar ratio solutions. The pH of each solution was adjusted to 6.0−6.5 by adding an appropriate amount of $(CH_3)_4NOH$ solution. The BNPP solution was then added to each solution, and the final pH was adjusted by adding an appropriate amount of buffer stock solution and used within 30 min after preparation. MES, MPS, TAPS, CHES, CAPS, and CABS with the respective pK_a values of 6.1, 7.2, 8.4, 9.3, 10.4, and 10.7 were used to prepare buffer solutions with the desired pH values. The final BNPP concentration was kept at 0.10 mM, and the lanthanide complex concentrations were 1.0 mM or greater to fulfill pseudo-first-order reaction conditions. The ionic strength was adjusted to 0.1 M with $(CH_3)_4NCl$ unless otherwise specified. A HP 8453 UV−vis spectrophotometer was used to measure the absorption increase with time at 400 nm due to the formation of nitrophenolate ion after BNPP hydrolysis.[31,34] Pseudo-first-order rate constants were calculated using the initial rate method or the integral method. A Sigmaplot was used for curve fitting.

Results

To establish a reference for comparison, we have determined the rates for the base-catalyzed BNPP hydrolysis reaction at [NaOH] = 0.033−0.166 M. Figure s1 (Supporting Information) shows that the plot of the observed rate constants vs [NaOH] is linear and that the calculated first-order rate constant, k_{OH}, is 2.30×10^{-5} M^{-1} s^{-1} using the relationship $k_{obs} = k_{OH}[OH^-]$. For all of the other studies, controlled BNPP hydrolysis reactions using only the buffer solutions without lanthanide complexes were always studied as references and the rates were all negligible.

Effects of pH. Figure 1 shows the plots of k_{obs} vs pH for the three Ln(III)−DO2A complexes, Ln = La, Eu, and Yb. The corresponding data are listed in Table 1 together with those of $EuK21DA^+$, $EuEDDA^+$, and EuHEDTA. For all three of the lanthanide complexes, the k_{obs} values increase with increasing pH. This is not the effect of increasing $[OH^-]$ or buffer reagents. According to the data of BNPP hydrolysis by NaOH discussed previously, for pH 11, that is, when $[OH^-] = 0.001$ M, the k_{obs} for OH^- catalysis would be 2.30×10^{-5} (M^{-1} s^{-1}) × 0.001 M or 2.30×10^{-8} s^{-1}, which is negligible as compared to the k_{obs} data in the presence of the lanthanide complexes.

Previously, we reported that the hydrolysis constant pK_h for $Eu(DO2A)(H_2O)_3^+$ was 8.1 ± 0.3.[46] The product after hydrolysis, $Eu(DO2A)(H_2O)_2(OH)$, is believed to be the reactive one. Thus, the rate "jump" for $EuDO2A^+$ at pH 8.1 is more likely because of the formation of the hydrolysis product. Assuming that the active species of all the lanthanide complexes studied are in the deprotonated $LnL(H_2O)_x(OH)$ form, the rate of each reaction can be expressed as

$$\text{rate} = k_{obs}[\text{BNPP}] = k_{LnL(OH)}[\text{LnL(OH)}][\text{BNPP}] \quad (1)$$

where $k_{LnL(OH)}$ is the apparent rate constant due to LnL(OH). Thus, $k_{obs} = k_{LnL(OH)}[\text{LnL(OH)}]$. If K_h is denoted as the coordinated water hydrolysis constant of $LnL(H_2O)$, then $K_h = \{[\text{LnL(OH)}][H^+]\}/[\text{LnL}(H_2O)]$, and the total lanthanide complex concentration is $[\text{LnL}]_t = [\text{LnL}(H_2O)] + [\text{LnL(OH)}]$. After substitution and rearrangement, the following expression is obtained

$$k_{obs} = \frac{k_{LnL(OH)}K_h[\text{LnL}]_t}{K_h + [H^+]} \quad (2)$$

Fitting the data points related to the first-rate "jump" listed in Table 1 to the expression of eq 2 using a nonlinear least-squares method gives the values of K_h and $k_{LnL(OH)}$, and the

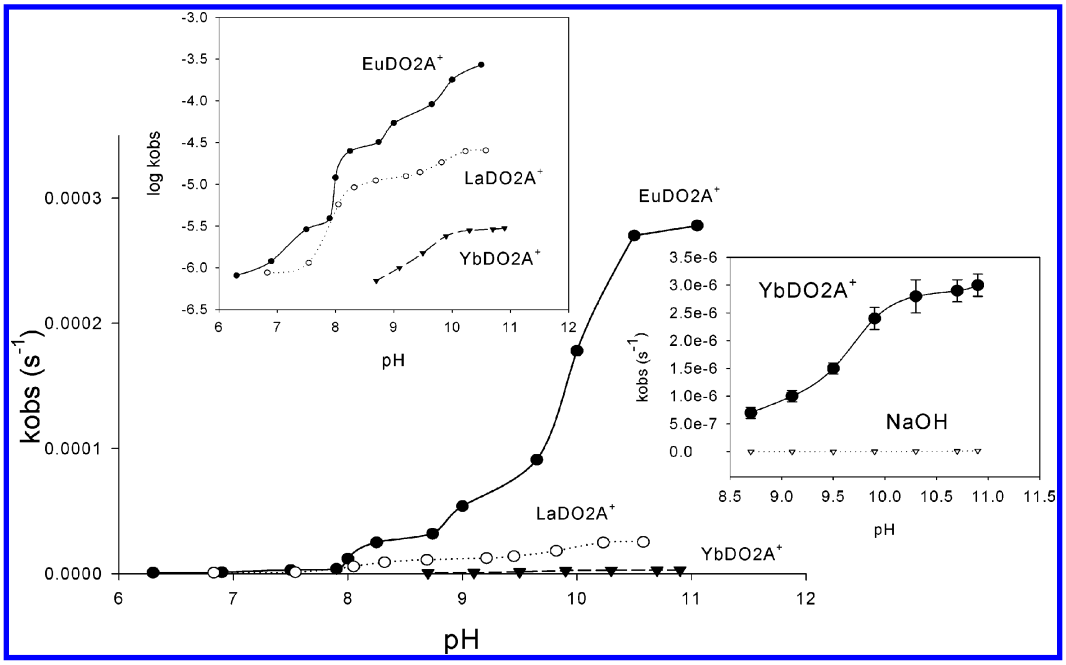

Figure 1. Plots of the observed BNPP hydrolysis rate constants vs pH by EuDO2A^{+} (●), LaDO2A^{+} (○), and YbDO2A^{+} (▼): [LnL] = 1.0 mM and [BNPP] = 0.10 mM, at 25 °C, μ = 0.10 $(CH_3)_4NCl$. Upper-left insert shows the logarithmic plots. Right insert shows YbDO2A^{+} (●) data vs buffer/NaOH (▼) k_{obs} data plots.

Table 1. Observed BNPP Hydrolysis Rate Constants vs pH by EuDO2A^{+}, LaDO2A^{+}, and YbDO2A^{+}, EuK21DA^{+}, EuEDDA^{+}, and EuHEDTA[a]

EuDO2A^{+}		LaDO2A^{+}		YbDO2A^{+}		EuK21DA^{+}		EuEDDA^{+}		EuHEDTA	
pH	k_{obs}	pH	k_{obs}	pH	k_{obs}	pH	k_{obs}	pH	k_{obs}	pH	k_{obs}
11.05	2.78×10^{-4}	10.58	2.54×10^{-5}	10.90	3.00×10^{-6}	9.90	1.33×10^{-7}	8.40	8.80×10^{-5}	11.90	4.01×10^{-5}
10.62	2.68×10^{-4}	10.23	2.49×10^{-5}	10.70	2.90×10^{-6}	9.10	1.28×10^{-7}	7.60	1.10×10^{-5}	11.42	4.05×10^{-5}
10.30	1.97×10^{-4}	9.82	1.83×10^{-5}	10.30	2.80×10^{-6}	8.50	1.01×10^{-7}	7.50	6.40×10^{-6}	10.95	3.86×10^{-5}
10.00	1.78×10^{-4}	9.45	1.39×10^{-5}	9.90	2.40×10^{-6}	8.03	7.48×10^{-8}	7.00	6.60×10^{-7}	10.50	3.22×10^{-5}
9.76	9.45×10^{-5}	9.21	1.25×10^{-5}	9.50	1.50×10^{-6}	7.52	5.05×10^{-8}			9.81	1.46×10^{-5}
9.65	9.10×10^{-5}	8.69	1.11×10^{-5}	9.10	1.00×10^{-6}	7.01	1.45×10^{-8}			9.42	3.01×10^{-6}
9.50	8.80×10^{-5}	8.32	9.14×10^{-6}	8.70	7.00×10^{-7}	6.56	1.09×10^{-8}			8.92	1.54×10^{-6}
9.48	8.16×10^{-5}	8.05	5.74×10^{-6}							8.43	1.69×10^{-7}
9.23	7.46×10^{-5}	7.54	1.15×10^{-6}								
9.00	5.40×10^{-5}	6.83	8.74×10^{-7}								
8.74	3.20×10^{-5}										
8.33	2.20×10^{-5}										
8.00	1.20×10^{-5}										
7.75	1.17×10^{-5}										
7.50	2.90×10^{-6}										
6.90	1.20×10^{-6}										
6.30	8.10×10^{-7}										

[a] All [LnL] = 1.0 mM except [EuHEDTA] = 10.0 mM and [BNPP] = 0.10 mM, at 25 °C, μ = 0.10 $(CH_3)_4NCl$.

Table 2. Fitted K_h and $k_{LnL(OH)}$ Values for the BNPP Hydrolysis by Various Lanthanide Complexes[a]

complex	pK_h	$k_{LnL(OH)}$	R^2	pH range
EuDO2A^{+}	8.4 ± 0.3	4.67×10^{-2}	0.979	6.30−8.74
LaDO2A^{+}	8.4 ± 0.2	1.71×10^{-2}	0.969	6.83−8.69
YbDO2A^{+}	9.4 ± 0.3	3.03×10^{-3}	0.981	8.70−10.90
EuK21DA^{+}	7.8 ± 0.1	1.31×10^{-4}	0.988	6.56−9.90
EuEDDA^{+}	9.0 ± 0.3[b]	4.00×10^{-1}	0.980	7.00−8.40
EuHEDTA	10.1 ± 0.2	4.10×10^{-3}	0.980	8.43−11.90

[a] All [LnL] = 1.0 mM except [EuHEDTA] = 10.0 mM and [BNPP] = 0.10 mM, at 25 °C, μ = 0.10 $(CH_3)_4NCl$. [b] The pK_a value for EuEDDA^{+} was obtained with only 4 data points and is expected to have larger relative error.

results are listed in Table 2. The fits are shown in Figure s2 (Supporting Information).

It is seen that the kinetic pK_h value for EuDO2A^{+} is 8.4 ± 0.3, which, within experimental error, matches the previously reported value of 8.1 ± 0.3 using a laser-excited fluorescence technique. It is noted that because of the possibility that there are other equilibria of the EuDO2A^{+} species, particularly at a high pH, that is, monomer−dimer equilibrium (vide infra), the pK_h value determined is a composite of multiple pH-dependent equilibria.[50,51] Similar arguments could be applied to LaDO2A^{+}, YbDO2A^{+}, and other Eu(III) complexes studied. The pK_h values for these lanthanide complexes are reasonable, however, few published data were available for comparison. The apparent rate constants due to LnL(OH), that is, $k_{LnL(OH)}$, are also obtained as the results of several equilibria and kinetic events associated with corresponding lanthanide complexes.

(50) Deal, A. K.; Burstyn, J. N. *Inorg. Chem.* **1996**, *35*, 2792−2798.
(51) Hegg, E. L.; Mortimore, H. S.; Cheung, C. L.; Huyett, J. E.; Powell, D. L.; Burstyn, J. N. *Inorg. Chem.* **1999**, *38*, 2961−2968.

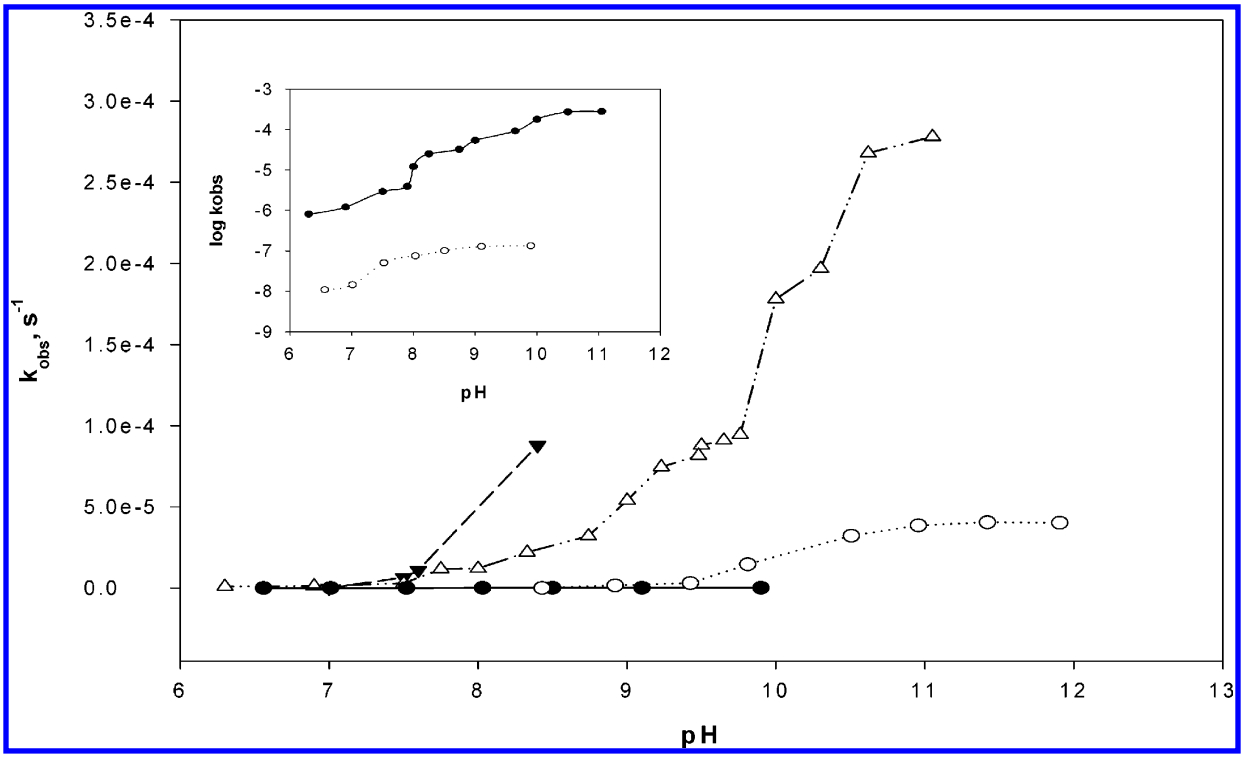

Figure 2. Plots of the observed BNPP hydrolysis rate constants vs pH by EuDO2A$^+$ (△), EuK21DA (●), EuHEDTA (○), and EuEDDA$^+$ (▼): 25 °C, μ = 0.10 M $(CH_3)_4NCl$, [EuDO2A$^+$] = [EuK21DA$^+$] = [EuEDDA$^+$] = 1.0 mM, [EuHEDTA] = 10 mM, [BNPP] = 0.10 mM, and [buffer] = 20 mM MES, MPS, TAPS, CHES, CAPS. The insert lines are log k_{obs} vs pH plots with EuDO2A$^+$ (●) and EuK21DA (○).

Further detailed analysis of the pH effects would require species distribution information for the hydroxo and possibly hydroxo-bridged complexes, particularly for data obtained at higher pH values. However, because of the sluggish complex formation and dissociation kinetic behavior of the macrocyclic DO2A complexes,[46,52,53] this information is difficult to obtain and will be reported and discussed at a later stage.[54] It is noted here that two sets of Ln(DO2A)$^+$ stability constants have been reported on the basis of different experimental conditions, and some rationalization will be discussed in a later contirbution.[54]

Effects of Metal Ionic Radii. Schneider et al. have reported the hydrolysis of phenyl phosphate esters and of DNA by uncomplexed lanthanide salt solutions.[29] At 25 °C and pH 7.0, the observed pseudo-first-order BNPP hydrolysis rates showed a saturation kinetics behavior as lanthanide ion concentration was increased. With the exception of Lu^{3+} and Yb^{3+}, the catalytic rate constants derived from the saturation kinetics correlate well with the ionic diameter of the cations and are independent of the underlying coordination numbers. This is consistent with an earlier study by Breslow et al. on the effects of metal ions on the cleavage of ribonucleotides and RNA model compounds.[16]

Our results showed that the observed BNPP hydrolysis rate constants with EuDO2A$^+$ were about 1.4−10 times greater than those with LaDO2A$^+$ in the pH range of 6.8−10.6, presumably as a result of the greater charge density of EuDO2A$^+$ (Figure 1). The LaDO2A$^+$ and EuDO2A$^+$ complexes are nine-coordinate,[46] and the YbDO2A$^+$ complex is eight-coordinate.[52] The remaining coordination sites would be occupied by three and two water molecules for the respective La/EuDO2A$^+$ and YbDO2A$^+$ complexes, assuming that DO2A occupies six donor sites. The lanthanide ion, Yb^{3+}, having a smaller ionic radius and greater charge density, is expected to have a lower pK_h value for the coordinated water molecule and therefore forms a better nucleophile, $(Yb{-}OH)^{2+}$. However, when Yb^{3+} is complexed by DO2A, the BNPP hydrolysis rates were found to be the lowest among the three DO2A complexes. This reduced reactivity of YbDO2A$^+$ toward BNPP hydrolysis may be a result of either fewer inner-sphere coordinated water molecules or other reasons such as inactive dimer formation (vide infra).

Effects of the Number of Inner-Sphere Coordinated Water Molecules. Figure 2 shows the plots of the observed BNPP hydrolysis rate constants vs pH by reactions with EuDO2A$^+$, EuK21DA$^+$, EuEDDA$^+$, and EuHEDTA. The three lanthanide complexes, EuDO2A$^+$, EuK21DA$^+$, and EuEDDA$^+$, were studied to examine the effects of the number of inner-sphere coordinated water molecules on the BNPP hydrolysis rates. This idea originates from the finding of Morrow et al. that the La(TCMC)$^{3+}$ with two inner-sphere coordinated water molecules promotes rapid cleavage of RNA oligomers but Eu(TCMC)$^{3+}$ or Dy(TCMC)$^{3+}$ with one inner-sphere coordinated water molecule does not, where TCMC is 1,4,7,10-tetrakis (carbomylmethyl)-1,4,7,10-tetraazacyclododecane, capable of octadentate coordination with

(52) Yerly, F.; Dumnand, F. A.; Toth, E.; Figueirnha, A.; Kovacs, Z.; Sherry, A. D.; Geralds, C. F. G. C.; Merbach, A. E. *Eur. J. Inorg. Chem.* **2000**, 1001−1006.
(53) Huskens, J.; Torres, D. A.; Kovacs, Z.; Andre, J. P.; Geraldes, C. F. G. C.; Sherry, A. D. *Inorg. Chem.* **1997**, *36*, 1495−1503.
(54) Wu, B.-H.; Chang, C. A. *Inorg. Chem.* **2005**. In press.

trivalent lanthanide ions.[18] Replacement of an amide group of TCMC by a noncoordinating nitrobenzyl group results in the heptadentate NBAC, that is, 1-(4-nitrobenzyl)-4,7,10-tris(carbomylmethyl)-1,4,7,10-tetraazacyclododecane. The monomeric Eu(NBAC)$^{3+}$ is then active in RNA cleavage (at pH 7.4).[26]

Laser-excited fluorescence studies confirmed that EuDO2A^{+} and EuK21DA^{+} have three and two inner-sphere coordinated water molecules,[43,46] respectively. The complex, EuEDDA^{+}, with the four donor atoms provided by EDDA, is assumed to have five inner-sphere coordinated water molecules. The observed BNPP hydrolysis rate constants with EuDO2A^{+} were about 74−1300 times greater than those of EuK21DA^{+} in the pH range of 6.5−9.9. At a lower pH range, EuEDDA^{+} has the greatest rates among the three complexes. Thus, it is appropriate to preliminarily conclude that, if the complexes remain monomeric (vide infra), then the more inner-sphere coordinated water molecules, the faster the phosphodiester hydrolysis rates. Unfortunately, at high pH, EuEDDA^{+} solution forms precipitates and prevents further studies. (This further demonstrated that complexation is important to control catalyst stability and reactivity.)

The overall basicity for DO2A is greater than that of K21DA.[41,46] DO2A also has a more rigid macrocycle with a smaller cavity and greater lanthanide complex formation stability than that of K21DA. On one hand, the higher basicity of DO2A may reduce the Lewis acidity of Eu^{3+}, increase the coordinated water pK_h value, and reduce the Eu(III)−OH^{-} nucleophilicity. On the other hand, the Eu^{3+} ion may be positioned deeper in the bigger macrocyclic cavity of K21DA and reduce the tendency of substrate binding. In addition, dimer formation is statistically more likely with LnDO2A^{+} than with LnK21DA^{+} which, depending on the final dimeric structure, results in more active or inactive species toward BNPP hydrolysis. The observed results of the current study seem to indicate that ligand basicity is not as important as the factors involving the number of inner-sphere coordinated water molecules and the steric effect imposed by the macrocyclic ligand.

Effects of the Charge of the Metal Complexes. Both EuDO2A^{+} and EuHEDTA have six donor ligands and three coordinated water molecules. However, the former has one positive charge and the latter has zero net charge. From Figure 2, it is observed that the promoted BNPP hydrolysis rates are greater for EuDO2A^{+} as expected because the phosphodiester substrates are negatively charged. The rate "jump" for EuHEDTA between pH 9.0 and 11.0 probably indicates that the hydrolysis constant of EuHEDTA is around 10.1. A more thorough analysis of the rates vs complex concentration reveals that the more reactive structure for EuDO2A^{+} is in a dinuclear form (vide infra) and EuHEDTA does not form a dimer[54] in the pH range studied. A detailed mechanistic analysis will be reported in the future.

Effects of the Concentrations of the Metal Complexes. Preliminary studies on the effects of concentrations of metal complexes were performed to elucidate possible reaction mechanisms. At pH 9.35, the rate−concentration (1.0−4.75 mM) data for EuDO2A^{+} were obtained and are shown in Figure 3, and it was clear that the relationship was more than first-order dependence.

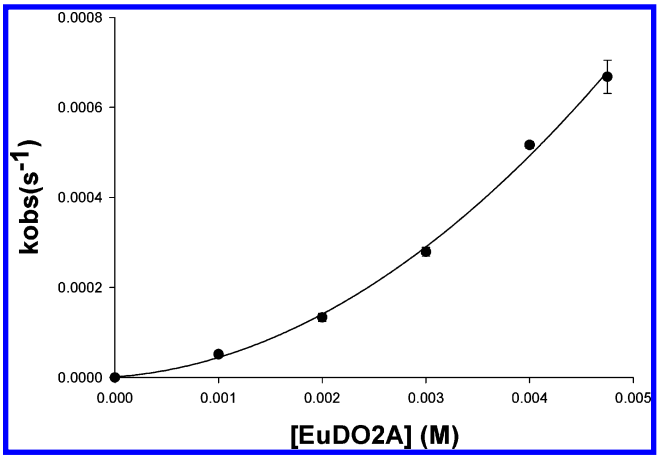

Figure 3. Dependence of pseudo-first-order rate constant on the concentration of EuDO2A^{+} at 25 °C, pH 9.35, 20 mM, CHES buffer, μ = 0.5 M $(CH_3)_4NCl$, and [BNPP] = 0.10 mM. The line was calculated by fitting the data to the Scheme 3 model.

Scheme 2. Simple Monomer Reaction Model

$$EuDO2A^{+} + BNPP \xrightarrow{k_1} P$$

$$2\,EuDO2A^{+} + BNPP \xrightarrow{k_2} P$$

$$Rate = k_1[EuDO2A^{+}]\,[BNPP] + k_2[EuDO2A^{+}]^2\,[BNPP]$$

$$k_{obs} = k_1[EuDO2A^{+}]_T + k_2[EuDO2A^{+}]_T^2$$

The data were initially fit into the simple monomer, two-pathways reaction model described in Scheme 2, and a second-order rate constant k_1 = 0.017 (±0.016) $M^{-1}\,s^{-1}$ and a third-order rate constant k_2 = 26.6 (±3.2) $M^{-2}\,s^{-1}$ (r^2 = 0.997) were obtained.

The relative fitting error was much smaller for the third-order rate constant as compared to that of the second-order (i.e., 12% vs 94%). Thus, it is likely that the third-order pathway is more important. For example, for [EuDO2A^{+}] = 1.0 mM, the calculated second- and third-order k_{obs} contributions were 1.7×10^{-5} and 2.66×10^{-5} s^{-1}, respectively, with the third-order rate being 1.6-fold faster than that of the second-order. However, this model was not a good one considering the collision theory because the probability for a three-body collision should be less than that of a two-body collision.

Because of the relatively high charge density of trivalent lanthanide ions, they are more prone to form hydrate-bridged, hydroxo-bridged, or oxo-bridged species at high pH[58] such as pH 9.35. These bridged species with more than one lanthanide ion Lewis acid center tend to hydrolyze the coordinated water molecules, making the resulting OH^{-} a more reactive nucleophile. Therefore, a more appropriate monomer−dimer reaction model is proposed in Scheme 3. The difference between this model and that shown in Scheme 2 is that there is a monomer−dimer equilibrium with a EuDO2A^{+} dimer formation equilibrium constant K_f.

To fit the data to the Scheme 3 model, we have followed that developed by Burstyn et al.[50,51] Assuming that in solution the Eu(III)-containing species are only the monomer

Scheme 3. Monomer−Dimer Reaction Model

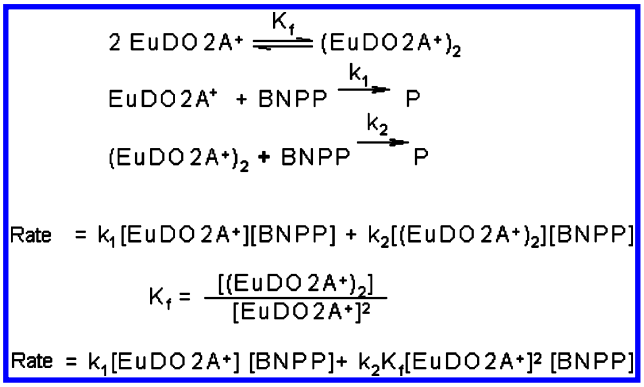

$EuDO2A^+$ and dimer $(EuDO2A^+)_2$, their concentrations can be derived by the following equations. The $EuDO2A^+$ concentration can be obtained as eq 4 by solving the quadratic eq 3. To simplify the treatment, it is assumed that $0.25 \ll 2K_f[Eu^{3+}]$, and eq 5 is obtained.

$$[Eu^{3+}]_T = [EuDO2A^+] + 2[(EuDO2A^+)_2]$$

$$K_f = \frac{[(EuDO2A^+)_2]}{[EuDO2A^+]^2}$$

$$[Eu^{3+}]_T = [EuDO2A^+] + 2K_f[EuDO2A^+]^2$$

$$2K_f[EuDO2A^+]^2 + [EuDO2A^+] - [Eu^{3+}]_T = 0 \quad (3)$$

$$[EuDO2A^+] = \frac{-1 + (1 + 8K_f[Eu^{3+}]_T)^{1/2}}{4K_f}$$

$$= \frac{-0.5 + (0.25 + 2K_f[Eu^{3+}]_T)^{1/2}}{2K_f} \quad (4)$$

Assumption: $0.25 \ll 2K_f[Eu^{3+}]_T$

$$[EuDO2A^+] = \frac{-0.25 + (2K_f[Eu^{3+}]_T)^{1/2}}{2K_f} \quad (5)$$

Substituting eq 5 into the rate law equation, we obtain eq 6.

$$k_{obs} = k_1\left(\frac{-0.5 + (2K_f[Eu^{3+}]_T)^{1/2}}{2K_f}\right) + k_2K_f\left(\frac{-0.5 + (2K_f[Eu^{3+}]_T)^{1/2}}{2K_f}\right) \quad (6)$$

Letting $[Eu]_T$ be X, k_{obs} be Y, monomer BNPP hydrolysis rate constant be $k_1 = a$, dimer formation constant be $K_f = b$, and dimer BNPP hydrolysis rate constant be $k_2 = c$, we obtain a $[Eu]_T$ polynomial (eq 7).

$$Y = a\left(\frac{-0.5 + (2bX)^{1/2}}{2b}\right) + bc\left(\frac{-0.5 + (2bX)^{1/2}}{2b}\right)^2$$

or

$$Y = \frac{-0.25a + 0.0625c}{b} + \frac{a - 0.5c}{2^{1/2}b^{1/2}}X^{1/2} + \frac{c}{2}X \quad (7)$$

Fitting the data to eq 7 using the Sigmaplot software showed that there were some discrepancies between the calculated and the experimental values at $[Eu]_T$ below 0.001 M which were not desirable. Thus, it was probably not appropriate to make the assumption that $0.25 \ll 2K_f[M^{n+}]_T$. When $[M^{n+}]_T = 0.001$ M, the calculated $2K_f[M^{n+}]_T$ value was 2.44, and 0.25 is not very small when compared to this value.

If the assumption is omitted, substituting eq 4 into the rate law, eq 8 is obtained.

$$k_{obs} = k_1\left(\frac{-0.5 + (0.25 + 2K_f[Eu^{3+}]_T)^{1/2}}{2K_f}\right) + k_2K_f\left(\frac{-0.5 + (0.25 + 2K_f[Eu^{3+}]_T)^{1/2}}{2K_f}\right) \quad (8)$$

Fitting the data to eq 8, it gives $k_1 = 9.1 \times 10^{-3}$ M^{-1} s^{-1}, $k_2 = 4.0$ M^{-1} s^{-1}, and $K_f = 8.2$ M^{-1} ($r^2 = 0.997$). The dimer rate constant k_2 is about 400 times greater than the monomer rate constant k_1. However, the small K_f value indicates that the dimer concentration is relatively small for a $[EuDO2A^+]$ range of 1.00−4.75 mM. The calculated monomer and dimer concentrations in the concentration range $[Eu^{3+}]_T = 1.00$−4.75 mM are shown in Figure 4.

Discussion and Conclusion

Design of Efficient Trivalent Macrocyclic Lanthanide Complexes for Phosphodiester Bond Hydrolysis. For monomeric trivalent macrocyclic lanthanide complex systems, it seems clear that a complex with a smaller lanthanide ionic radius (i.e., greater ionic potential), a greater number of inner-sphere coordinated water molecules, and a higher positive complex charge operating at higher pH would be the more effective one for phosphodiester bond hydrolysis. The coordination number, cavity size, and steric constraint of the macrocyclic ligand may have dominant effects on the resulting phosphodiester bond hydrolysis rates promoted by the lanthanide complex. However, these requirements might need major modifications if dimer, tetramer, or higher-order oligomers are formed.

Effects of Dimer, Tetramer, or Higher-Order Oligomer Formation. Schneider attributed the unusual catalyst concentration effects in the hydrolysis of phenyl phosphodiesters of the heavier lanthanides to cation clustering which leads to diminished activities.[29] It is possible that at pH 7.0, Yb^{3+} could form hydroxo-bridged dimers and higher order clusters. For $YbDO2A^+$, it is highly possible that the smaller Yb^{3+} ion is deeply located in the DO2A macrocycle and only two coordinated water molecules were present. One indirect support for such a proposition was the fact that $EuDOTA^-$ has only one coordinated water molecule and $EuTETA^-$ has none.[55,56] The crystal structural data confirmed that the Eu^{3+} ion is indeed located deeper in the 14-membered TETA pocket than that of the DOTA pocket, with the respective Eu−N-plane distances of 1.15 and 1.50 Å.[55,56] Our prelimi-

(55) Chang, C. A.; Francesconi, L. C.; Malley, M. F.; Kumar, K.; Gougoutas, J. Z.; Tweedle, M. F.; Lee, D. W.; Wilson, L. J. *Inorg. Chem.* **1993**, *32*, 3501−3508.
(56) Spirlet, M.-R.; Rebizant, J.; Loncin, M.-F.; Desreux, J. F. *Inorg. Chem.* **1984**, *23*, 4278−4283.

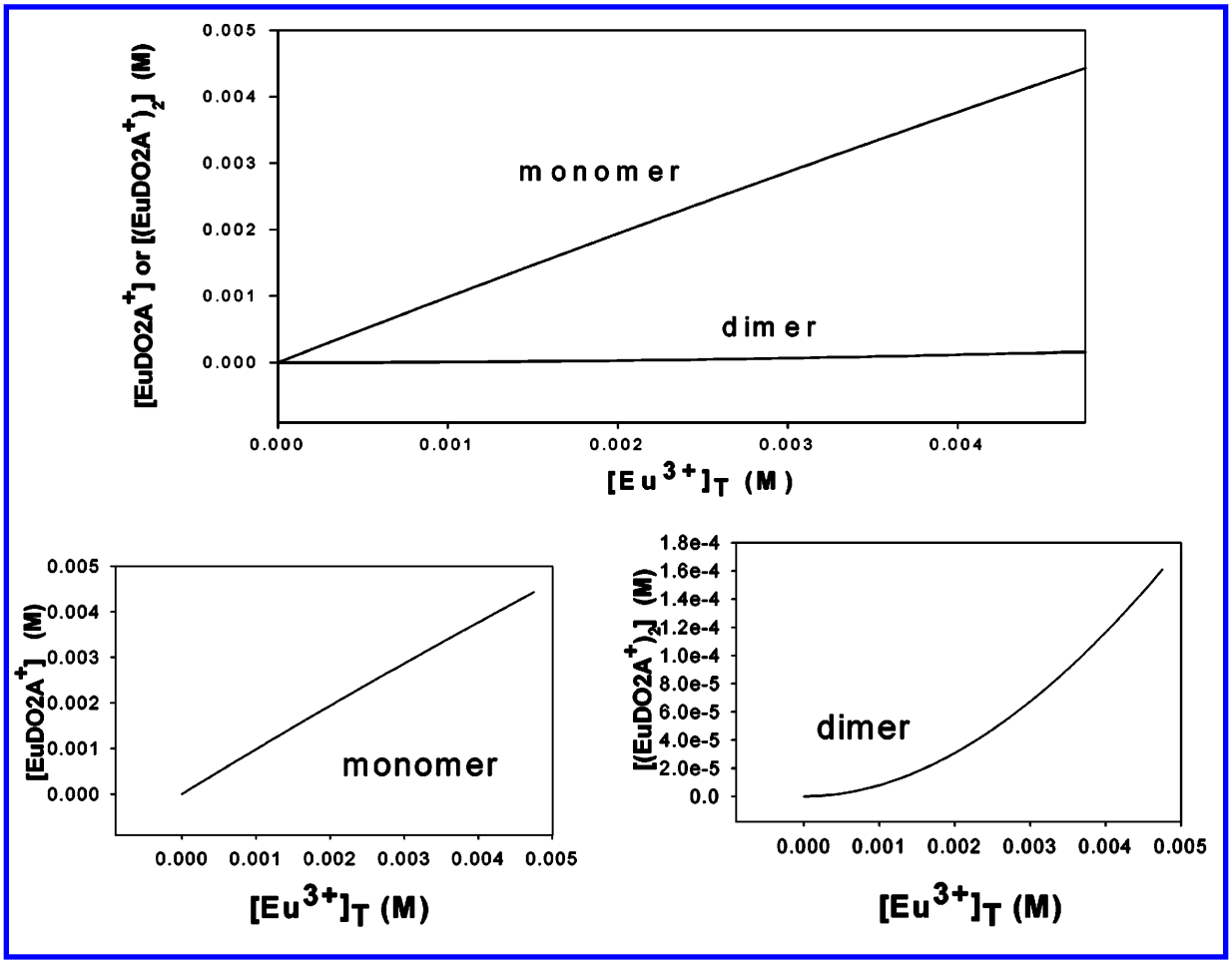

Figure 4. [Monomer] and [dimer] when $[Eu^{3+}]_T = 1.00-4.75$ mM and $K_f = 8.2$.

Scheme 4. Active and Inactive Dimer of $LnDO2A^+$ for Phosphodiester Bond Hydrolysis

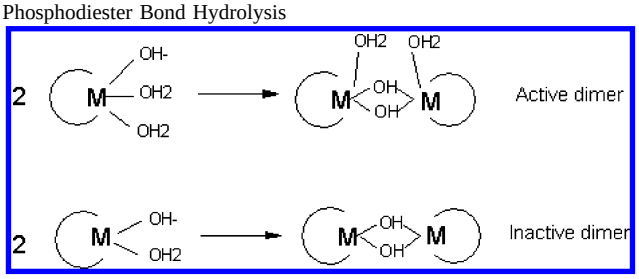

nary study of the effects of the concentrations of the metal complexes on BNPP hydrolysis also indicated that the more reactive structure of $EuDO2A^+$ is dimeric.[54] A recent spectroscopic study of the hydration state of Ln(DO2A)-$(H_2O)_n^+$ concluded a decrease in the inner-sphere water coordination number from $n = 3$ (Ce−Eu), to $n = 2$ (Tb−Yb).[52] Assuming that $YbDO2A^+$ is eight-coordinate with two inner-sphere coordinated water molecules, the resulting dimer formation would render $[Yb(DO2A)(\mu\text{-}OH)]_2$ inactive as shown in Scheme 4. This is because the two bridged hydroxide ions are tightly bound to the Yb^{3+} ions and coordination unsaturation space is not available on Yb^{3+} for BNPP substrate binding for further hydrolysis. A similar argument was also presented for Cu^{2+} complexes.[50,51,57] On the other hand, the $EuDO2A^+$ complex with three inner-sphere coordinated water molecules would form a hydroxo-bridged active dimer with two remaining inner-sphere coordinated water molecules for BNPP substrate binding as depicted also in Scheme 4. Thus, it is interesting to note that the dimeric hydroxo-bridged active species $[Eu(DO2A)(H_2O)(\mu\text{-}OH)]_2$ originally with three coordinated water molecules on each monomer exert faster BNPP hydrolysis rates than the inactive dimeric species $[Yb(DO2A)(\mu\text{-}OH)]_2$ originally with two coordinated water molecules on each monomer.

It is noted that only recently a series of studies concerning ligand-controlled self-assembly of polynuclear lanthanide−oxo/hydroxo complexes have been reported for potential applications on catalytic cleavage of RNA or DNA molecules.[58−60] Many of these clusters are formed by core components of crystallographically characterized dinuclear and tetranuclear cubane-like lanthanide−hydroxo species. These structures are normally obtained at low pH values (i.e., pH 4−6), but even more novel structures have been obtained at "high" pH values (i.e., pH > 6).[61] For example, at pH ≥

(57) Deck, K. M.; Tseng, T. A.; Burstyn, J. N. *Inorg. Chem.* **2002**, *41*, 669−677.
(58) Zheng, Z. *J. Chem. Soc., Chem. Commun.* **2001**, 2521−2529.
(59) Wang, R.; Carducci, M. D.; Zheng, Z. *Inorg. Chem.* **2000**, *39*, 1836−1837.
(60) Zheng, X.-J.; Jin, L.-P.; Gao, S. *Inorg. Chem.* **2004**, *43*, 1600−1602.
(61) Wang, R.; Zheng, Z.; Jin, T.; Staples, R. *Angew. Chem., Int. Ed.* **1999**, *38*, 1813−1815.

13, $K_4[(EDTA)Er(\mu\text{-}OH)_2Er(EDTA)]$ has been isolated from a reaction mixture of $Na[Er(EDTA)(H_2O)_2]$ and KOH.[58] The core component of the dinuclear Er(III)−EDTA complex is exactly the abovementioned inactive dimer form (Scheme 4). The fact that the hydroxo-bridged Er(III)−EDTA formation requires higher pH indicates that the intermediate is the formation of $[Er(EDTA)(H_2O)(OH)]^{2-}$ and the pK_h of the negatively charged $[Er(EDTA)(H_2O)_2]^-$ is probably close to 12−13. (Note that the respective pK_h values for $EuEDTA^-$ and $YbEDTA^-$ are 12.48 and 12.3[62].) All of these are consistent with what we have discussed so far. Moreover, macrocyclic ligands with certain steric controls might add some new design dimensions on the physiochemical or biochemical properties of the resulting lanthanide complexes, such as faster water exchange rates for magnetic resonance imaging contrast agent applications[63] or various cluster formation structures for phosphate ester bond hydrolysis. In fact, studies involving $[Ln(NO2A)]^+$ (where Ln = Eu(III) and Yb(III) and NO2A = 1,7-dicarboxymethyl-1,4,7-triazacyclononane) reveal both similar and different BNPP hydrolysis rate behaviors as compared with $[Ln(DO2A)]^+$, and the results will be reported at a later stage.[64]

Future Studies. The observations and discussions presented by this initial publication on macrocyclic lanthanide complexes as artificial nucleases and ribonucleases, such as (1) relatively faster BNPP hydrolysis rates promoted by $EuDO2A^+$ at high pH, (2) a different trend of $LnDO2A^+$-promoted BNPP hydrolysis reaction rates (as compared to free lanthanide salt solutions), (3) variation of lanthanide hydrolysis pK_h values upon complexation, and (4) possible dimeric or higher-order lanthanide metal ion cluster involvement in BNPP hydrolysis at high pH, all warrant more detailed studies. In addition, this study also reveals that, with the exception of the crystal structures, the equilibrium as well as the kinetics of hydroxo-bridged lanthanide complex cluster formation has not been carefully studied. We are in the process of obtaining more data to answer the abovementioned questions, and further details will be reported soon.

Acknowledgment. We wish to thank the National Science Council of the Republic of China (Taiwan) for financial support (Grant No. NSC-93-2113-M-009-004) of this work.

Supporting Information Available: Plots of the observed rate constants vs [NaOH] and pH, respectively, for BNPP hydrolysis. This material is available free of charge via the Internet at http://pubs.acs.org.

IC0485458

(62) Southwood-Jones, R. V.; Merbach, A. E. *Inorg. Chim. Acta* **1978**, *30*, 77−82.
(63) Congreve, A.; Parker, D.; Gianolio, E.; Botta, M. *J. Chem. Soc., Dalton Trans.* **2004**, 1441−1445.
(64) Chang, C. A.; Lin, J.-J. Unpublished results.